ORIGINAL ARTICLE

Spatial distribution of the protist community in the southern part of the Okhotsk Sea off Hokkaido during summer

Yusuke Hamao[1] · Kohei Matsuno[1,2] · Yoko Mitani[3,4] · Atsushi Yamaguchi[1,2]

Abstract

The southern part of the Okhotsk Sea off Hokkaido has rich fishery resources supported by high primary production. The phytoplankton community has been described by several studies based on size-fractionated chlorophyll *a* concentration and primary production; however, the details of the species composition of nano- and micro-protist communities have not been well investigated. We evaluated the spatial distribution and relationship with hydrography of nano- and micro-protist communities in the southern region of the Okhotsk Sea off Hokkaido during the summer of 2019. Forty-two species of diatoms from 19 genera, dinoflagellates from 7 genera, tintinnid ciliates, oligotrich ciliates, and 1 genus of silicoflagellates were identified. Their spatial distribution showed distinct differences among the taxa. Cluster analysis based on the protist cell density identified six groups with geographically well-distinguished distributions. Diatom-dominant communities were distributed in the Cold Water Belt and Soya warm current along the coastal area of Hokkaido. Nanoflagellate-dominated communities were distributed in the offshore area. Some harmful species of diatoms (*Pseudonitzschia pseudodelicatissima*) and dinoflagellates (*Alexandrium* spp.) were dominant in the Cold Water Belt off Wakkanai. We suggest that the upwelling of cold water could increase the abundance of harmful species, with immanent negative impacts on marine ecosystems or fishery resources. In summary, the species composition and abundance of the summer protist community was strongly related to different water masses in the southern part of the Okhotsk Sea off Hokkaido.

Keywords Diatoms · Dinoflagellates · Ciliates · Nanoflagellates · Okhotsk Sea · Cold Water Belt · Harmful algae

1 Introduction

The southern part of the Okhotsk Sea off Hokkaido is known as one of the important fishing grounds in Japan due to abundant fishery resources, such as scallops and salmon (Kasai et al. 2017; Sakurai 2011; Shiomoto et al. 2018). At higher trophic levels (sea birds and marine mammals), this region

✉ Yusuke Hamao
  hamayu-5362@eis.hokudai.ac.jp

1 Faculty/Graduate School of Fisheries Sciences,
   Hokkaido University, 3-1-1 Minato-cho, Hakodate,
   Hokkaido 041-8611, Japan

2 Arctic Research Center, Hokkaido University, Kita-21
   Nishi-11 Kita-ku, Sapporo, Hokkaido 001-0021, Japan

3 Field Science Center for Northern Biosphere, Hokkaido
   University, 20-5 Benten-Cho, Hakodate, Hokkaido 040-0051,
   Japan

4 Present Address: Wildlife Research Center, Kyoto University,
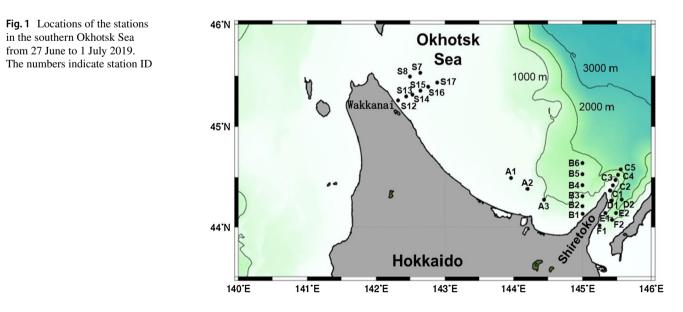   2-24 Tanaka-Sekiden-cho, Sakyo, Kyoto 606-8203, Japan

is also an important foraging habitat (Kazama et al. 2018). In summer, this area is characterized by three different water masses: the warm and saline Soya Warm Current (SWC) distributed in the coastal region, the less-saline Fresh Surface Okhotsk Sea Water (FSOSW) observed in the surface layer of the offshore region, and low-temperature Intermediate Cold Water (ICW) distributed in the lower layer (Takizawa 1982). In addition, the Cold Water Belt (CWB) is distributed between the SWC and FSOSW during summer and autumn along the southern part of the Okhotsk Sea off Hokkaido (Ishizu et al. 2006, 2008; Kuma et al. 2014; Mitsudera et al. 2011). Because the water in the CWB is composed of a mixture of high iron concentration SWC and upwelling high-nutrient ICW (Ishizu et al. 2008), high primary production is observed even in summer, resulting in rich fishery resources (Mustapha et al. 2009) and much prey for sea birds (e.g., short-tailed shearwaters and northern fulmar) on the coast of the Okhotsk Sea in Hokkaido (Tanaka and Kajihara 1979).

The high primary production in this area during the sea-ice-free seasons has been revealed by previous studies based

on size-fractionated chlorophyll *a* concentration (Chl. *a*), and the ^{13}C isotope-labeling method in incubation experiments (Kasai et al. 2010; Kasai and Hirakawa 2015; Shiomoto 2011; Shiomoto et al. 2018). From July to October, assemblages of the larger size fraction (> 10 μm) dominate more in coastal regions than in the offshore regions (Kasai et al. 2010; Kasai and Hirakawa 2015). Near the Shiretoko Peninsula, in late spring to early summer and in late summer to early autumn, the proportion of the larger fraction (> 10 μm) is high on the western side of the peninsula, whereas the proportion of the smaller fraction (< 2 μm) is high on the eastern side (Shiomoto 2011). In terms of species composition of nano- and micro-protists, harmful dinoflagellates and diatoms are described in the Okhotsk Sea (e.g., Shimada et al. 2010; Kasai and Hirakawa 2015). Many investigations have been performed on *Alexandrium tamarense,* among the harmful dinoflagellates, as it causes the accumulation of paralytic shellfish toxin (PST) (e.g., Shimada et al. 2010; Shimada 2017). In diatoms, changes in species composition between warm and cold waters have been revealed (Kasai and Hirakawa 2015). Spring diatom blooms are composed mainly of *Thalassiosira nordenskioeldii*, *Thalassiosira gravida*, *Thalassiosira eccentrica*, and *Chaetoceros subsecundus* in coastal surface water (Sorokin and Sorokin 1999). In the winter season *Odontella aurita* and *Thalassiosira* spp. are dominant species (McMinn et al. 2008). However, in contrast to the availability of information about Chl. *a* and primary productivity, the species composition of nano- and micro-protists during summer is not well described, and spatial variation in nano- and micro-protists, which are also important as primary producers, is not well understood.

In the present study we investigated the spatial distribution of nano- and micro-protist communities off Wakkanai and around the Shiretoko Peninsula during summer to clarify their relationship with the hydrological environment. In particular, we focused on the CWB off Wakkanai and a comparison of the east and west sides of the Shiretoko Peninsula, which possess the characteristic features of this area, to evaluate the effects of physical and chemical features of the environment on the nano- and micro-protist communities.

2 Materials and methods

Conductivity–Temperature–Depth (CTD; Sea-Bird SBE-911 plus) casts were conducted at 28 stations (located at 44–46° N, 142–146° E) in the southern part of the Okhotsk Sea off Hokkaido between June 27 and July 1, 2019, on T/S Oshoro-Maru (Fig. 1, Supplementary Table 1). Line transects were established along each of the eight sets of stations; we termed the transects L1–L8 in sequence from the northwestern to the southeastern parts (Fig. 2a). Water samples (1 L) were collected from the surface and the layer of maximum Chl. *a* (range of 10–35 m in depth) using a plastic bucket and Niskin rosette water sampler mounted on the CTD frame. The samples were fixed with 1% glutaraldehyde immediately. Seawater samples for measurement of Chl. *a* and nutrient contents were collected from the same layers as the fixed samples. Water samples (250 mL) were filtered using Whatman GF/F filters for the measurement of Chl. *a*. After filtration, the filters were immersed in 6 mL of *N,N*-dimethylformamide under dark conditions for 24 h, and then, Chl. *a* concentration was measured using a fluorometer (10-AU, Tuner Designs, Inc.) (Holm-Hansen et al. 1965). The water samples for nutrient analyses were frozen and stored at − 80 °C onboard. Nutrient concentrations (nitrate, nitrite, phosphate, and silicate) were measured using
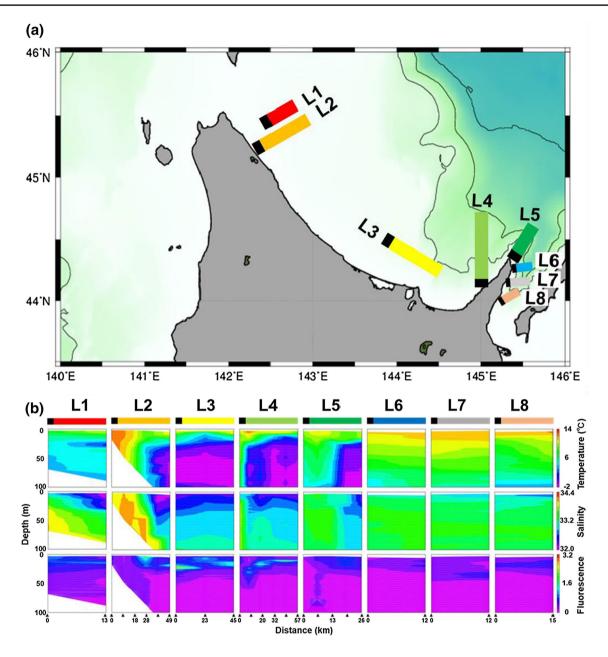

Fig. 1 Locations of the stations in the southern Okhotsk Sea from 27 June to 1 July 2019. The numbers indicate station ID

Fig. 2 Eight transects (L1–L8) in the southern Okhotsk Sea from June 27 to July 1, 2019. **a** Cross-sectional distribution of temperature, salinity, and fluorescence at each transect. **b** Solid triangles at the bottom indicate sampling stations at each transect

an autoanalyzer (QuAAtro 2HR, BL-TEC) in a land-based laboratory.

In the land-based laboratory the fixed samples (1 L) were stored on a flat table for more than 1 day to allow the phytoplankton cells to settle at the bottom of the bottle. Afterwards, the samples were concentrated to 20 mL using a siphon. Subsamples (500 µL) of the concentrated sample were mounted on a glass slide using a micropipette. Phytoplankton cells were identified and enumerated using an inverted microscope (Eclipse-TE200, Nikon) at 40–600 × magnification. Diatoms, dinoflagellates, and

silicoflagellates were identified to the lowest possible levels (species or genus) according to the methods proposed by Hasle and Syvertsen (1997), Horner (2002), and Karen (1997). Tintinnid ciliates and oligotrich ciliates were counted separately. Nanoplankton (size range was 4.8–12.6 µm) were also counted, but their cell densities might have been underestimated due to their small size. All of the nanoflagellates were classified as autotrophic/mixotrophic/heterotrophic, because we did not use epifluorescence microscopy to check whether the cells had chloroplasts. Cell counting was performed with a maximum of 300 cells per subsample. After

counting, we calculated the abundances of each taxon in the sample (cells L^{-1}).

The abundances (X: cells L^{-1}) for all of the taxa were fourth root transformed ($X^{1/4}$) prior to the statistical analyses to reduce any bias in the estimations of abundance (Quinn and Keough 2002). Similarities between the nano- and micro-protist samples were calculated using the Bray–Curtis similarity index, and then, a dendrogram was created using the unweighted pair group method using the arithmetic mean (UPGMA). Nonmetric multidimensional scaling (NMDS) ordination was performed to distribute the groups onto a two-dimensional map. Pearson regression analyses were performed using environmental data (temperature; salinity; sampling depth; fluorescence; and Chl. a, nitrate + nitrite, phosphate, and silicate concentrations) as dependent variables to clarify the significance of their relationships to the cluster groups. Cluster analysis and NMDS were performed using PRIMERv7 (PRIMER-E Ltd.). Intergroup differences between each of nano- and micro-protists (abundance of each species or taxon) and hydrography data were tested using one-way ANOVA and Tukey–Kramer post hoc test using Statview (SAS Institute Inc.).

3 Results

3.1 Spatial distribution in hydrography

Along L2, high temperatures (> 10 °C) were observed at depths of < 20 m on the inshore side, whereas low temperatures (2 °C) were observed at depths of > 20 m on the offshore side (Fig. 2). Similarly, cold water (< 2 °C) was distributed on the offshore sides of L3, L4, and L5. However, at L6–L8 located on the eastern side of the Shiretoko Peninsula, warm water above 10 °C was generally observed at depths of < 20 m, but no cold water prevailed. Salinity showed a similar distribution to temperature (Fig. 2). On the coastal side of L2, high salinity (33.6–34.2) was found throughout the water column. Low salinity (32.2–32.4) was observed at a depth of < 30 m on the offshore side. The cold water in L3–L5 showed slightly low salinity at approximately 32.4. At L6–L8, salinity was higher than that on the western side (L3–L5). Fluorescence was extremely low through the study area, but relatively high values were observed at depths of 0–30 m in L2–L4, especially at the surface in the middle area along L2.

The CWB was indicated by observations of the horizontal distribution of temperature being 2–3 °C lower (observed in patches at the surface) compared to surrounding water; the CWB was observed at Stations S8 and S15 off Wakkanai, which demonstrated high Chl. a concentration (Fig. 3). The CWB separated warm and saline water in the inshore area from cold and fresh water in the offshore area. In addition,
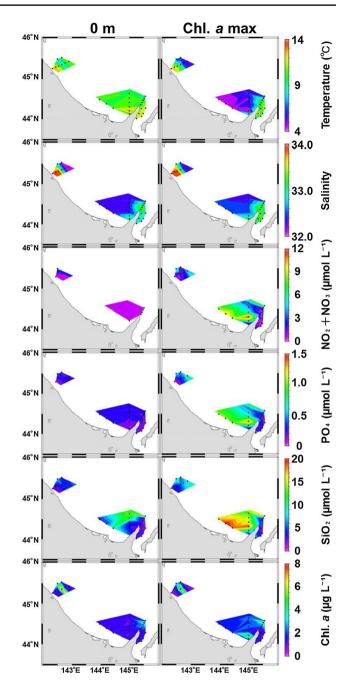

Fig. 3 Horizontal distribution of chlorophyll a and nutrients at the surface (left panel) and chlorophyll a maximum depth (right panel) in the southern Okhotsk Sea from June 27 to July 1, 2019

highly saline water was distributed off Wakkanai and around the Shiretoko Peninsula. The concentrations of nitrate and nitrite ranged from 0.11 to 11.64 µmol L^{-1} at the surface and in the maximum Chl. a layer (Fig. 3). Almost all surface water showed low concentrations of nitrate and nitrite compared to the maximum Chl. a layer. In the maximum Chl. a layer, the highest concentrations of nitrate and nitrite were observed at Station B3 in the western side of the

Shiretoko Peninsula. By contrast, extremely low concentrations of nitrate and nitrite (close to zero) were observed in the coastal areas off Wakkanai and on the central and eastern sides of the Shiretoko Peninsula. Phosphate and silicate concentrations ranged from 0.09 to 1.37 μmol L^{-1} and 1.34 to 20.14 μmol L^{-1}, respectively, and exhibited horizontal patterns similar to those of nitrate and nitrite. Chl. a ranged from 0.53 to 7.63 μg L^{-1} and showed a similar distribution between the surface and the maximum Chl. a layer; the highest value was observed at Station S15 in the CWB off Wakkanai, and relatively high concentrations were observed in the western and central areas of offshore Shiretoko Peninsula.

3.2 Spatial distribution of the protists

Diatoms and nanoflagellates were dominant among the protists throughout the study area in terms of cell density (Fig. 4). High abundances ($> 5.0 \times 10^4$ cells L^{-1}) of diatoms were observed in the CWB (at Stations S8 and S15). Around the Shiretoko Peninsula, diatom abundance was high on the western side and central areas ($> 5.0 \times 10^4$ cells L^{-1}) and low on the eastern side in both 0 m and maximum Chl. a layers. The total abundance of dinoflagellates ranged from 3.3×10^2 to 6.25×10^4 cells L^{-1}, and their distribution pattern contrasted to the distribution of diatoms. Off Wakkanai, the abundance of dinoflagellates was higher offshore ($> 1.0 \times 10^4$ cells L^{-1}) and lower near the coast. Around the Shiretoko Peninsula, their abundance was low on the western side and high ($> 1.0 \times 10^4$ cells L^{-1}) on the central and eastern sides. The total ciliate abundance was lower than those of diatoms and dinoflagellates, ranging from 2.45×10^2 to 8.93×10^3 cells L^{-1}, and distributed at similar densities throughout the study area. The nanoflagellate abundance ranged from 3.27×10^3 to 8.93×10^4 cells L^{-1} and nanoflagellates was the most dominant taxon at several stations. High abundances, above 1.0×10^4 cells L^{-1}, were observed in both layers in most areas but were slightly lower at Stations S7 and S17 off Wakkanai.

3.3 Relationship between protist community and hydrography

In this study, 42 species of diatoms in 19 genera, 7 genera of dinoflagellates, tintinnid ciliates, oligotrich ciliates, and 1 genus of silicoflagellates were observed (Table 1). The cluster analysis using abundance separated the protist communities into six groups (A–F) at 57% similarity (Fig. 5a). Group A, distributed off Wakkanai (Fig. 5c), had the lowest total abundance (3.86×10^4 cells L^{-1}) and was dominated by dinoflagellates (Fig. 5b), especially *Alexandrium* spp. (Table 1). Group B was mostly distributed offshore around the Shiretoko Peninsula and was dominated by
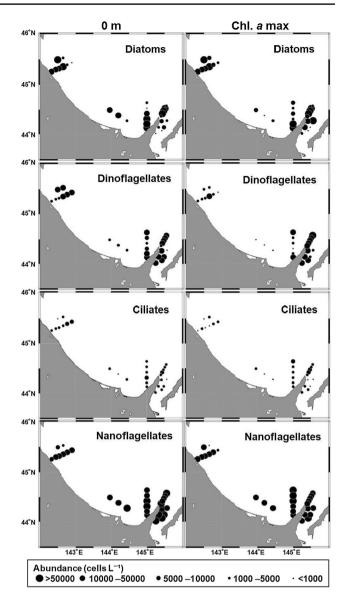

Fig. 4 Horizontal distributions of diatoms, dinoflagellates, and nanoflagellates in abundance at the surface (left panel) and chlorophyll *a* maximum depth (right panel) in the southern Okhotsk Sea from June 27 to July 1, 2019

nanoflagellates. *Dictyocha* spp. and unidentified dinoflagellates were the characteristic species in this group. Group C occurred locally near the Shiretoko Peninsula and was dominated by nanoflagellates with no characteristic species. Group D, distributed mostly on the surface from L3 to around the Shiretoko Peninsula, was characterized by abundant nanoflagellates and low abundances in several species of *Chaetoceros* spp. Group E was locally distributed off Wakkanai and was dominated by diatoms. Some species of *Chaetoceros* spp., *Pseudonitzschia pseudodelicatissima* and *Pleurosigma normanii* were characteristic of this group (Table 1). Group F, which occurred widely from off Wakkanai to the eastern side of the Shiretoko Peninsula, showed the

Table 1 Comparison of nano- and micro-protist abundance among the groups identified using cluster analysis (cf. Fig. 5) in the southern Okhotsk Sea from June 27 to July 1, 2019

Species	Mean abundance (cell L^{-1})						One-way ANOVA	Tukey–Kramer test
	A (5)	B (11)	C (2)	D (14)	E (2)	F (21)		
Diatoms								
Asterionellopsis glacialis	0	0	0	0	0	384	NS	
Asterionellopsis kariana	0	0	0	0	0	14	NS	
Bacteriastrum delicatulum	0	0	0	0	0	62	NS	
Bacteriastrum furcatum	0	0	0	0	0	6	NS	
Bacteriastrum hyalinum	29	0	0	0	0	0	NS	
Chaetoceros affinis	0	123	143	1834	12,569	11,577	***	B² C² D² D² F¹ E¹
Chaetoceros atlanticus	0	0	0	22	0	0	NS	
Chaetoceros concavicornis	0	290	143	266	0	212	NS	
Chaetoceros convolutus	2288	979	0	2419	0	1538	NS	
Chaetoceros criophilus	0	0	0	0	0	5	NS	
Chaetoceros curvisetus	0	0	0	0	0	12	NS	
Chaetoceros danicus	0	0	106	36	858	629	**	D² C^{1,2} F¹ E¹
Chaetoceros debilis	0	0	0	0	1348	1738	**	Not detected
Chaetoceros decipiens	29	0	0	47	245	1000	NS	
Chaetoceros diadema	0	0	573	259	1151	1269	*	Not detected
Chaetoceros didymus	0	0	0	6	0	941	**	D² D² F¹
Chaetoceros furcellatus	0	0	0	201	5584	1146	***	D² F² E¹
Chaetoceros laciniosus	147	0	96	2527	6154	12,623	***	C² A² D² E^{1,2} F¹
Chaetoceros radicans	0	0	0	184	0	905	NS	
Chaetoceros socialis	0	0	0	2139	25,105	16,345	***	A² D² E¹
Chaetoceros teres	0	0	0	0	0	273	NS	
Corethron hystrix	40	1	153	943	0	992	NS	
Coscinodiscus centralis	0	0	0	0	0	28	NS	
Cylindrotheca closterium	137	5	354	82	819	1096	*	B² D² A^{1,2} C^{1,2} E^{1,2} F¹
Dactyliosolen fragilissimus	55	0	141	141	0	1605	*	A² C² D²
Eucampia zodiacus	0	0	0	15	0	249	NS	
Fragilariopsis atlantica	0	0	0	0	0	5	NS	
Fragilariopsis pseudonana	0	22	106	0	0	84	NS	
Guinardia flaccida	0	0	0	0	0	135	NS	
Leptocylindrus danicus	0	222	430	519	3599	5506	***	B² C² D² E^{1,2} F¹
Leptocylindrus minimus	93	65	0	0	0	1595	NS	
Merosira arctica	0	0	0	0	0	142	NS	
Navicula spp.	16	0	176	0	0	24	NS	
Paralia sulcata	0	4	0	0	0	0	NS	
Pleurosigma normanii	0	5	0	3	490	81	***	B² D² F² E¹

Table 1 (continued)

Species	Mean abundance (cell L^{-1})						One-way ANOVA	Tukey–Kramer test
	A (5)	B (11)	C (2)	D (14)	E (2)	F (21)		
Pseudo-nitzschia fraudulenta	0	0	50	278	1234	7321	*	Not detected [E1]
Pseudo-nitzschia pseudodelicatissima	14	0	0	42	21,391	1867	***	A2 D2 F2 [E1]
Pseudo-nitzschia pungens	0	0	525	0	0	254	NS	
Skeletonema costatum	0	0	0	0	0	46	NS	
Thalassionema nitzschioides	28	347	2068	304	0	3488	***	A2 D2 B2 C1,2 [F1]
Thalassiosira eccentrica	0	0	78	0	0	0	***	Not detected
Thalassiosira nordenskioeldii	0	0	0	0	823	215	NS	
Thalassiosira pacifica	0	0	0	4	0	335	NS	
Total diatoms	2875	2064	5143	12,271	81,368	75,744	***	B2 A2 C2 D2 F1 [E1]
Dinoflagellates								
Alexandrium spp.	11,057	134	126	373	18,663	6523	***	C2 B2 D2 F1,2 A1 [E1]
Ceratium fusus	0	21	0	50	0	22	NS	
Ceratium spp.	0	34	0	13	0	0	NS	
Dinophysis spp.	152	8	0	39	0	133	NS	
Prorocentrum spp.	1024	0	96	197	1234	348	**	C2 D2 F1,2 A1 [E1]
Protoperidinium spp.	14	24	0	104	0	340	*	A2 B2 D1,2 [F1]
Pyrophacus spp.	0	103	0	0	0	150	NS	
Unidentified dinoflagellates	4820	19,978	9980	4424	0	9381	*	D2 A1,2 C1,2 F1,2 [B1]
Total dinoflagellates	17,066	20,302	10,201	5202	19,897	16,896	NS	
Ciliates								
Tintinnid ciliates	515	1390	863	1121	328	1156	NS	
Oligotrich ciliates	3810	1916	2001	1600	0	1755	*	D2 F1,2 B1,2 C1,2 [A1]
Total Ciliates	4325	3306	2864	2721	328	2910	NS	
Dictyocha spp.	224	992	20	226	0	27	**	C2 F2 A2 D2 [B1]
Nanoflagellates	14,072	52,596	45,208	44,074	11,928	23,735	***	E2 A2 F2 D1 C1 [B1]
Total	38,562	79,261	63,437	64,495	113,522	119,314	**	A2 C2 D2 E1,2 B1,2 [F1]

Differences among the groups were tested using one-way ANOVA and post hoc Tukey–Kramer tests. Any groups not connected by the superscript numbers on the groups were significantly different ($p < 0.05$). Values are means. Numbers in parentheses are the number of stations belonging to each group

NS: not significant
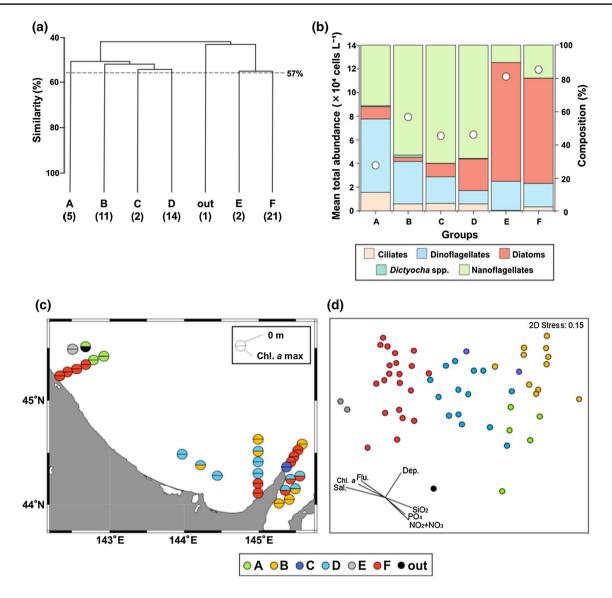
*: $p < 0.05$

**: $p < 0.01$

***: $p < 0.001$

Fig. 5 Results of cluster analysis based on nano- and micro-protist abundance in the southern Okhotsk Sea from June 27 to July 1, 2019. **a** Six groups (A–F) were identified using the Bray–Curtis similarity connected with UPGMA. Mean abundance and species/taxon composition of each group **b** Horizontal distribution of the six groups in the southern Okhotsk Sea during June 27 and July 1, 2019. **c** Nonmetric multidimensional scaling plots of the six groups. **d** The direction and length of the lines indicate the relationship to groups and the strength of the relationship. Dep.: depth, Flu.: fluorescence, Chl. : chlorophyll *a*, Sal.: salinity.

highest abundance (1.19×10^5 cells L^{-1}) and was dominated by diatoms. *Chaetoceros* spp., *Dactyliosolen fragilissimus*, and *Leptocylindrus dannicus* were characteristic species of diatoms in this group.

Each group was clearly separated in the NMDS plot (Fig. 5d). The environmental parameters that showed significant relationships ($p < 0.05$) with the protist community included sampling depth; salinity; fluorescence; and Chl. *a*, silicate, phosphate, and nitrate + nitrite concentrations (Fig. 5d). One-way ANOVA showed that the environmental factors that differed among the groups were salinity and nitrate + nitrite and silicate concentrations (Table 2). Salinity

and nutrient concentrations showed opposite trends. Groups C and F had high salinity and low nutrient concentrations, whereas groups B, D, and E had low salinity and high nutrient concentrations.

The protist groups are shown on a T–S diagram to depict the relationships between the protist communities and water mass categories (Fig. 6). We categorized the water mass off Wakkanai and around the Shiretoko Peninsula during summer as SWC (temperature = 7–20 °C, salinity = 33.6–34.3), FSOSW (temperature ≤ 18 °C, salinity ≤ 32.5) or ICW (temperature = − 1.8 to 2 °C, salinity = 32.8–33.4) according to Takizawa (1982).

Table 2 Comparison of the environmental factors among the groups identified using cluster analysis (cf. Fig. 5) in the southern Okhotsk Sea from June 27 to July 1, 2019.

Parameters	Groups						One-way ANOVA	Tukey–Kramer test
	A (5)	B (11)	C (2)	D (14)	E (2)	F (21)		
Temperature (°C)	8.2±2.49	8.4±2.80	9.2±0.31	9.2±2.99	6.9±0.78	10.3±2.35	NS	
Salinity	32.2±0.11	32.7±0.36	33.2±0.05	32.6±0.27	33.1±0.27	33.3±0.43	***	A[3] D[2,3] E[2,3] B[2,3] C[1,2] F[1]
Chl. a (µg L^{-1})	1.2±0.34	1.5±0.47	1.1±0.32	1.3±0.41	3.4±1.03	2.5±2.01	*	Not detected
NO$_2$+NO$_3$ (µmol L^{-1})	3.3±2.08	4.4±3.48	1.7±1.40	8.7±2.45	5.4±2.59	1.1±1.86	***	F[2] C[2] B[1,2] A[1,2] E[1,2] D[1]
PO$_4$ (µmol L^{-1})	0.36±0.24	0.46±0.28	0.37±0.11	0.44±0.42	0.5±0.14	0.21±0.19	NS	
SiO$_2$ (µmol L^{-1})	5.7±2.08	10.2±6.40	4.7±1.81	8.4±1.81	9.2±1.90	3.5±0.58	*	F[2] C[1,2] A[1,2] D[1,2] E[1,2] B[1]

Differences among the groups were tested using one-way ANOVA and post hoc Tukey–Kramer tests. Any groups not connected by the superscript numbers on the groups were significantly different ($p<0.05$). Values are means (±SD). Numbers in parentheses are the number of stations belonging to each group

NS: not significant
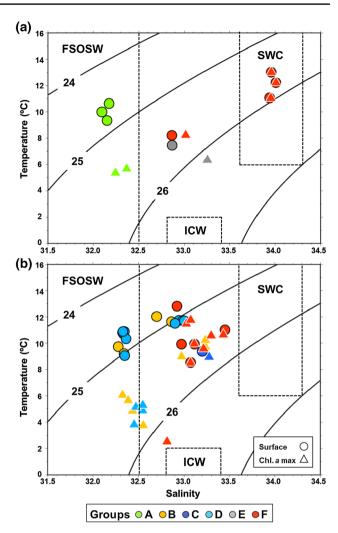
*: $p<0.05$

**: $p<0.01$

***: $p<0.001$

Fig. 6 Temperature–salinity diagram showing the six groups identified from the Bray–Curtis similarity (cf. Figure 5a) around the Wakkanai (**a**) and Shiretoko Peninsulas (**b**) (cf. Figure 1) in the southern Okhotsk Sea from June 27 to July 1, 2019. Circle and triangle frames for each symbol indicate the water was collected from the surface or chlorophyll a maximum depth, respectively. SCW: Soya Warm Current, FSOSW: Fresh Surface Okhotsk Sea Water, ICW: Intermediate Cold Water (cf. Takizawa et al. 1982).

Off Wakkanai, Group A plotted below 32.5 on salinity, which indicated that the group was strongly influenced by FSOSW. Group F was under the SWC with a salinity markedly above 33.6, except at a few stations (Fig. 6a). Group E, locally distributed off Wakkanai, was plotted in the middle of groups A and F. Around the Shiretoko Peninsula, some of groups B and D were plotted below 32.5 on salinity and categorized in the FSOSW (Fig. 6b). However, most of groups C and F were in mixed temperatures between 8 and 14 °C and mixed salinities between 32.5 and 33.6.

4 Discussion

Through the sampling region, nano- and micro-protist communities were roughly divided into two groups (Fig. 5a and b) with clear spatial patterns; a diatom-dominated group (including group E and F) in coastal areas and a nanoflagellates-dominated group (including groups A, B, C and D) in offshore areas (Fig. 5c). The diatom-dominated group mainly occurred in the water mass categorized as SWC and some occurred in the mixed area between SWC and FSOSW, whereas the nanoflagellates-dominated group was mainly seen in FSOSW (Fig. 6). This division was strongly related to several hydrographic features (Fig. 5d). The diatom-dominated group was located at high Chl. *a* and low nutrient concentration (NMDS plot, Fig. 5d) suggesting that diatoms were able to grow in the season previous to our sampling using the nutrients then available. By contrast, the nanoflagellates-dominated group occurred alongside relatively high nutrients (Table 2 and Fig. 5d), but where the large-sized phytoplankton abundance was low. This mis-matched relationship may be due to low iron concentration in the offshore waters (Kudo et al. 2011; Kuma et al. 2014). According to Kudo et al. (2011), iron concentration is low in the FSOSW in this area during summer. In addition, compared to large phytoplankton, small phytoplankton are more able to grow under low iron concentrations due to their low iron requirement (Brand et al. 1983; Sunda and Huntsman 1995; Timmermans et al. 2001). Thus, the difference in iron requirement of nanoflagellates and diatoms could induce the dominance of nanoflagellates in offshore areas, where iron concentrations are low (Kudo et al. 2011; Kuma et al. 2014). In the southern part of the Okhotsk Sea off Hokkaido during summer we propose that the different hydrographic features of the water masses (including their nutrients and iron concentrations) influence the distribution of protist communities.

4.1 Effect of the CWB on the protist community off Wakkanai

Off Wakkanai, the protist communities were clearly divided between coastal and offshore regions; groups E and F with high diatom abundance were observed along the coast, whereas group A with the lowest abundance was seen offshore (Fig. 5b and c). The CWB off Wakkanai is colder and with a higher Chl. *a* distribution during summer (Ishizu et al. 2006; Mitsudera et al. 2011). Group E occurred in waters that were slightly cooler and with higher Chl. *a* than those, where groups A and F occurred (Table 2 and Fig. 6), so group E in this study could be categorized as a CWB community.

There are currently two hypotheses regarding the mechanism of formation of the CWB: one is that the cold water at the bottom in the SWC is continuously vertically advected to the surface (Ishizu et al. 2006), and the other is that the cold water at the bottom near the Soya Strait upwells and then horizontally advects off Wakkanai (Iida et al. 2018; Mitsudera et al. 2011). In the former case, the upwelling cold water is considered to be the ICW that exists below the SWC and FSOSW during the summer. According to Ishizu et al. (2008), the water in the CWB is not composed of a specific water mass and is described as consisting of a mixture of SWC, FSOSW, and ICW. By contrast, in the latter case, the upwelling cold water is considered to be Japan Sea Intermediate Water (JSIW). Although the physical processes involved in the formation of the CWB are still under discussion, both the ICW and the JSIW have been reported to have high nutrient concentrations (Kuma et al. 2014; Maita and Toya 1986). In this study, higher nitrate, phosphate, and silicate concentrations were observed in Station S8 than those observed for the surrounding waters (Fig. 3); this may have been caused by upwelling from the bottom layer.

Iron plays an important role in the metabolic processes of growth, photosynthesis, respiration, and nitrogen assimilation in marine phytoplankton (Behrenfeld and Milligan 2013; Twining and Baines 2013). Iron-limitation of phytoplankton growth would be expected to occur in coastal upwelling areas (Aguilar-Islas et al. 2007; Bruland et al. 2001; Gerringa et al. 2012; Hutchins et al. 2002; Sedwick et al. 2011). In this study area, dissolved iron concentrations are low in the FSOSW (< 1 nM) and ICW (0.5 nM) but high (> 1 nM) in the SWC during spring and summer, because of the supply of iron from the Asian continent via atmospheric dust and from rivers (Kudo et al. 2011; Kuma et al. 2014). Kudo et al. (2011) conducted incubation experiments to investigate the effects of these nutrients and iron concentrations on phytoplankton in the SWC, FSOSW, and ICW. They reported that large phytoplankton (> 10 μm, composed mainly of diatoms) dominated in the case of mixed ICW and SCW. Thus, the mixture of low nutrient, high iron concentration SWC and high nutrient, low iron concentration ICW provided suitable conditions for diatom growth, eventually forming the diatom-dominated group E.

As mentioned above, the CWB provides suitable conditions for diatom growth; thus, not only primary production but also production at higher trophic levels can be increased in the CWB (Mustapha et al. 2009). Group F showed high diversity in species composition, whereas group E was dominated by some harmful species. In particular, *Pseudonitzschia pseudodelicatissima* and *Alexandrium* spp. were, respectively, 11 and 2.9 times higher in group E than in group F. Since *P. pseudodelicatissima* has domoic acid in cells (Bates et al. 2018; Moschandreou et al. 2010), the grazing activity of copepods ceases for a while after grazing on it

(Tammikehto et al. 2012), which means that primary production cannot reach higher trophic levels. As an example of the negative impact, more than 100 sea birds (brown pelicans) died in 5 days, because they fed on mackerel contaminated by domoic acid-producing diatoms (*Pseudonitzschia* spp.) (Beltran et al. 1997). In addition, *Alexandrium* spp., including *A. tamarense* and *A. catenella,* cause paralytic shellfish toxin accumulation (PST). Therefore, the water in the CWB has potentially negative impacts on both marine ecosystems and fishery resources both directly and indirectly.

4.2 High abundance distribution of *Alexandrium* spp. off Wakkanai

The abundance of *Alexandrium* spp. was high in groups A and E off Wakkanai (Table 1). As mentioned above, group E was categorized as a CWB community, whereas group A had the lowest salinity and belonged to FSOSW. The area off Wakkanai is known as one of the important scallop fishing grounds of the world (Kosaka and Ito 2006), but PST occurs approximately once every 4 years and causes economic losses (Shimada et al. 2012). Due to the importance of *A. tamarense* as a cause of PST, it has been the subject of many investigations (e.g., by Shimada et al. (2010) and Shimada (2017)). The abundance of *A. tamarense* in late July was highest in the FSOSW, and *A. tamarense* blooms existed slightly offshore of the CWB (Miyazono and Minoda 1990; Shimada et al. 2012; Shimada 2017). These previously reported distribution patterns were similar to those seen herein. The growth of *A. tamarense* vegetative cells is limited when < 0.12 μM phosphate is available (Yamamoto and Tarutani 1999). *A. tamarense* is thought to be able to utilize nutrients in the lower layers by diel vertical migration (Lewis et al. 2006; MacIntyre et al. 1997). Lack of nutrients was unlikely to restrict the growth of *A. tamarense* in the regions, where groups A and E were observed, since phosphate concentrations were above 0.12 μM at the surface and at the layer of maximum Chl. *a*.

Alexandrium tamarense is known to have a life cycle in which the cysts (hypnozygotes, formed by sexual reproduction) germinate and produce planomeiocytes. Then, nursing cells asexually divide and proliferate by meiosis. Again, they produce motile planozygotes by sexual reproduction, and they become settling cysts and are dormant in the sediment (Ishikawa and Imai 2011; Shimada 2017). In the surface water of the Okhotsk Sea during summer, *A. tamarense* increases in "warm years" when the SWC is dominant and decreases in "cold years" when the ICW is dominant. This is because the cysts in the bottom sediment may germinate during the dominance of the SWC (Shimada 2017). Since the warm SWC flows as a submerged current near the bottom during spring (Aota 1975), the bottom temperature increases to the optimal temperature for germination of *A. tamarense*

cysts (5–21 °C) (Anderson 1998; Shimada 2017). Moreover, *A. tamarense* blooms near the CWB originate from Aniva Bay on southern Sakhalin Island (Orlova et al. 2004) and are transported along the front with the SWC (Oguma et al. 2011). Although we did not identify *Alexandrium* spp. to the species level in this study, the abundance and distribution of *Alexandrium* spp. were similar to those reported earlier, which suggests that the high temperature of the bottom layer due to the warm SWC and no nutrient limitation may facilitate the growth of *Alexandrium* spp.

4.3 Influence of the SWC on the protist community around Shiretoko Peninsula

In the Okhotsk Sea facing northeastern Hokkaido the warm and saline SWC flows along the coast, and the distribution of the SWC expands with increasing current speed from spring to summer (Aota 1975; Takizawa 1982). Numerical models have shown that the SWC on the north side of the Shiretoko Peninsula does not directly enter the east side of the peninsula (Mori et al. 2010) and that the flow path changes depending on the wind direction (Sato et al. 2006). In addition, based on field observations, the SWC flows into the subsurface layer (above 150 m depth, Oguma et al. 2007) on the east side of the peninsula (Sato et al. 2006). The diatom-dominated group F was widely distributed along the coastal area off Wakkanai and the eastern Shiretoko Peninsula in this study, in a distribution similar to that of the SWC (Fig. 5c). Specifically, group F was concentrated near the coast in the western and central areas of the Shiretoko Peninsula, and it occurred in the Chl. *a* maximum layer on the east side of the peninsula (Fig. 5c). Thus, since the distribution of group F coincided with the route of the SWC (Mori et al. 2010; Sato et al. 2006; Takizawa 1982), group F could be defined as an SWC community in this study.

4.4 East–west comparison across the Shiretoko Peninsula

In this study, differences in the protist community were observed between the eastern and western sides of the Shiretoko Peninsula; the diatom-dominated group F was seen on the western side, but on the eastern side, nanoflagellate-dominated groups B and D also occurred along with group F. As an example, a more detailed comparison at Station B1 (on the west side of the peninsula) shows that the contributions of diatoms and nanoflagellates to total abundance were 56% and 21%, respectively. By contrast, at Station F1 on the east side of the peninsula, the contributions of diatoms and nanoflagellates to total abundance were 0.9% and 82%, respectively. Even though our study did not report on < 2 μm phytoplankton, the east–west differences that we observed in the protist community were consistent with those of a previous study (Shiomoto

2011). According to Shiomoto (2011), since there was no clear difference in nutrient concentrations on either side of the peninsula, the west–east difference is potentially due to the strong predation pressure by zooplankton on large phytoplankton and weak predation pressure on small phytoplankton on the eastern side. However, in the current study we observed that the amounts of nutrients on the eastern side were significantly lower than those on the western side, especially in the zone of Chl. *a* maximum, which differs from the results of the previous study. This distribution of nutrients can be explained by the presence of the high-nutrient ICW (Maita and Toya 1986), observed at > 20 m depth in the western (L4) part of the peninsula. In general, it is well known that large phytoplankton require higher nutrient concentrations for growth than small phytoplankton (Sarthou et al. 2005). Therefore, we propose that the east–west difference in nutrient concentrations induced the differences in the protist community that we observed in this study.

5 Conclusion

There were distinct patterns in the spatial distribution of the protist community in the southern part of the Okhotsk Sea off Hokkaido. Diatoms dominated in the coastal areas, where the SWC was dominant or near the upwelling that develops the CWB. By contrast, nanoflagellates were dominant in the offshore areas. The toxic dinoflagellate *Alexandrium* spp. was abundant in the CWB and FSOSW. Thus, the distribution of the protists was largely governed by the different water masses in the southern part of the Okhotsk Sea off Hokkaido during summer.

References

Aguilar-Islas AM, Hurst MP, Buck KN, Sohst B, Smith GJ, Lohan MC, Bruland KW (2007) Micro- and macronutrients in the southeastern Bering Sea: insight into iron-replete and iron-depleted regimes. Prog Oceanogr 73:99–126

Anderson DM (1998) Physiology and bloom dynamics of toxic *Alexandrium* species, with emphasis on life cycle transitions. NATO ASI Ser G41:30–47

Aota M (1975) Studies on the Soya Warm current. Low Temp Sci A33:151–172 (**In Japanese with English summary**)

Bates SS, Hubbard KA, Lundholm N, Montresor M, Leaw CP (2018) *Pseudo-nitzschia, Nitzschia,* and domoic acid: new research since 2011. Harmful Algae 79:3–43

Behrenfeld MJ, Milligan AJ (2013) Photophysiological expressions of iron stress in phytoplankton. Annu Rev Mar Sci 5:217–246

Beltrán AS, Palafox-Uribe M, Grajales-Montiel J, Cruz-Villacorta A, Ochoa JL (1997) Sea bird mortality at Cabo San Lucas, Mexico: evidence that toxic diatom blooms are spreading. Toxicon 35:447–453

Brand LE, Sunda WG, Guillard RRL (1983) Limitation of marine phytoplankton reproductive rates by zinc, manganese, and iron. Limnol Oceanogr 28:1182–1198

Bruland KW, Rue EL, Smith GJ (2001) Iron and macronutrients in California coastal upwelling regimes: implications for diatom blooms. Limnol Oceanogr 46:1661–1674

Gerringa LJA, Alderkamp AC, Laan P, Thuroczy CE, DeBaar HJW, Mills MM, van Haren H, Arrigo KR (2012) Iron from melting glaciers fuels the phytoplankton blooms in Amundsen Sea (Southern Ocean): iron biogeochemistry. Deep Sea Res II 71–76:16–31

Hasle GR, Syvertsen EE (1997) Marine diatoms. In: Tomas CR (ed) Identifying marine phytoplankton. Academic Press, San Diego, pp 5–385

Holm-Hansen O, Lorenzen CJ, Holmes RW, Strickland JDH (1965) Fluorometric determination of chlorophyll. ICES J Mar Sci 30:3–15

Horner RA (2002) A taxonomic guide to some common marine phytoplankton. Biopress Limited, England, p 195

Hutchins DA, Hare CE, Weaver RS, Zhang Y, Firme F, DiTullio GR, Alm MB, Riseman SF, Maucher JM, Geesey ME, Trick CG, Smith GJ, Rue EL, Conn J, Bruland KW (2002) Phytoplankton iron limitation in the Humboldt current and Peru upwelling. Limnol Oceanogr 47:997–1011

Iida H, Isoda Y, Kobayashi N, Horio K (2018) Observations and model experiments of the diurnal eddy of the Cold Water Belt along the offshore side of the Soya Warm Current. Oceanogr Jpn 27:155–174 (**In Japanese with English abstract**)

Ishikawa A, Imai I (2011) Diversity of life cycles and life cycle strategies of microalgal flagellates. Bull Plankton Soc Jpn 58:60–64 (**In Japanese with English abstract**)

Ishizu M, Kitade Y, Matsuyama M (2006) Formation mechanism of the Cold-Water Belt formed off the Soya Warm Current. J Oceanogr 62:457–471

Ishizu M, Kitade Y, Matsuyama M (2008) Characteristics of the cold-water belt formed off Soya Warm Current. J Geophys Res 113:C12010. https://doi.org/10.1029/2008JC004786

Karen AS (1997) Marine Dinoflagellates. In: Tomas CR (ed) Identifying marine phytoplankton. Academic Press, San Diego, pp 387–584

Kasai H, Hirakawa K (2015) Seasonal changes of primary production in the south-western Okhotsk Sea off Hokkaido, Japan during the ice-free period. Plankton Benthos Res 10:178–186

Kasai H, Nakano Y, Ono T, Tsuda A (2010) Seasonal change of oceanographic conditions and chlorophyll *a* vertical distribution in the southwestern Okhotsk Sea during the non-iced season. J Oceanogr 66:13–26

Kasai H, Nagata R, Murai K, Katakura S, Tateyama K, Hamaoka S (2017) Seasonal change in oceanographic environments and the influence of interannual variation in the timing of sea-ice retreat on chlorophyll *a* concentration in the coastal water of northeastern Hokkaido along the Okhotsk Sea. Bull Coast Oceanogr 54:181–192 (**In Japanese with English summary**)

Kazama K, Nishizawa B, Tsukamoto S, Gonzalez JE, Kazama MT, Watanuki Y (2018) Male and female Black-tailed Gulls *Larus crassirostris* feed on the same prey species but use different feeding habitats. J Ornithol 159:923–934

Kosaka Y, Ito H (2006) Chapter 22 Japan. In: Shumway SE, Parson GJ (eds) Scallops: biology, ecology and aquaculture. Elsevier, Amsterdam, pp 1093–1141

Kudo I, Aya F, Takata H, Kobayashi N (2011) Oceanographic structure and biological productivity in the coastal area of Okhotsk Sea. Bull Coast Oceanogr 49:13–21 (**In Japanese with English abstract**)

Kuma K, Sasayama R, Hioki N, Morita Y, Isoda Y, Hirawake T, Imai K, Aramaki T, Nakamura T, Nishioka J, Ebuchi N (2014) Chemical evidence for the origin of the cold water belt along the northeastern coast of Hokkaido. J Oceanogr 70:377–387

Lewis NI, Xu W, Jericho SK, Kreuzer HJ, Jericho MH, Cembella AD (2006) Swimming speed of three species of *Alexandrium* (Dinophyceae) as determined by digital inline holography. Phycologia 45:61–70

MacIntyre JG, Cullen JJ, Cembella AD (1997) Vertical migration, nutrition and toxicity in the dinoflagellate *Alexandrium tamarense*. Mar Ecol Prog Ser 148:201–216

Maita Y, Toya K (1986) Characteristics on the distribution and composition of nutrients in subarctic regions. Bull Jpn Soc Fish Oceanogr 50:105–113 (**In Japanese with English abstract**)

McMinn A, Hattori H, Hirawake T, Iwamoto A (2008) Preliminary investigation of Okhotsk Sea ice algae; taxonomic composition and photosynthetic activity. Polar Biol 31:1011–1015

Mitsudera H, Uchimoto K, Nakamura T (2011) Physical oceanography of Soya Warm Current: mechanisms of the Cold Belt formation off the Soya Warm Current. Bull Coast Oceanogr 49:3–12 (**In Japanese with English abstract**)

Miyazono A, Minoda T (1990) Regional distribution of dinoflagellate population off the Coasts of Hokkaido in the Japan and Okhotsk Seas from spring to autumn, 1983. J Oceanogr Soc Jpn 46:96–106

Mori F, Isoda Y, Abe S, Kobayashi N, Yahaba H, Isogai Y (2010) Seasonal variations of surface flow patterns in the Nemuro Strait. Oceanogr Jpn 19:89–110 (**In Japanese with English abstract**)

Moschandreou KK, Papaefthimiou D, Katikou P, Kalopesa E, Panou A, Nikolaidis G (2010) Morphology, phylogeny and toxin analysis of *Pseudo-nitzschia pseudodelicatissima* (Bacillariophyceae) isolated from the Thermaikos Gulf, Greece. Phycologia 49:260–273

Mustapha MA, Saito S, Lihan T (2009) Satellite-measured seasonal variations in primary production in the scallop-farming region of the Okhotsk Sea. ICES J Mar Sci 66:1557–1569

Oguma S, Kawasaki Y, Azumaya T (2007) Water mass variation process in the Nemuro Strait during spring and autumn. Oceanogr Jpn 16:361–374 (**In Japanese with English abstract**)

Oguma S, Ono T, Watanabe YW, Kasai H, Watanabe S, Nomura D, Mitsudera H (2011) Flux of low salinity water from Aniva Bay (Sakhalin Island) to the southern Okhotsk Sea. Est Coast Shelf Sci 91:24–32

Orlova TY, Selina MS, Stonik IV (2004) Species structure of plankton microalgae on the coast of the Sea of Okhotsk on Sakhalin Island. Russ J Mar Biol 30:77–86

Quinn GP, Keough MJ (2002) Experimental design and date analysis for biologists. Cambridge University Press, New York, p 557

Sakurai Y (2011) Conservation of biodiversity and sustainable fisheries in the coastal marine ecosystems of the Shiretoko World Natural Heritage Site. Bull Coast Oceanogr 48:139–147 (**In Japanese with English abstract**)

Sarthou G, Timmermans KR, Blain S, Treguer P (2005) Growth physiology and fate of diatoms in the ocean: a review. J Sea Res 53:25–42

Sato M, Kono T, Kawasaki Y (2006) Inflow of Soya Warm Current induced by wind in the northern Nemuro Strait in summer. Oceanogr Jpn 16:455–470 (**In Japanese with English abstract**)

Sedwick PN, Marsay CM, Sohst BM, Aguilar-Islas AM, Lohan MC, Long MC, Arrigo KR, Dunbar RB, Saito MA, Smith WO, DiTullio GR (2011) Early season depletion of dissolved iron in the Ross Sea polynya: implications for iron dynamics on the Antarctic continental shelf. J Geophys Res 116:C12019. https://doi.org/10.1029/2010JC006553

Shimada H, Sawada M, Kuribayashi T, Nakata A, Miyazono A, Asami H (2010) Spatial distribution of the toxic dinoflagellate *Alexandrium tamarense* in summer in the Okhotsk Sea off Hokkaido. Plankton Benthos Res 5:1–10

Shimada H, Sawada M, Tanaka I, Asami H, Fukamachi Y (2012) A method for predicting the occurrence of paralytic shellfish poisoning along the coast of Hokkaido in the Okhotsk Sea in summer. Fish Sci 78:865–877

Shimada H (2017) Biological oceanographic study on method for predicting the occurrence of paralytic shellfish toxin along the Okhotsk Sea coast off Hokkaido. PhD thesis, Hokkaido University, Graduate School of Fisheries Sciences. https://doi.org/10.14943/doctoral.r7027 (**In Japanese with English summary**)

Shiomoto A (2011) Phytoplankton biomass and production in the coastal area of the Shiretoko Peninsula during late spring to early autumn: comparison between the Okhotsk Sea and the Nemuro Straight. Bull Coast Oceanogr 49:37–48 (**In Japanese with English abstract**)

Shiomoto A, Fujimoto Y, Mimura N, Sasaki A, Itoi D, Imasato S, Takahashi N, Takenaka Y, Fujita T (2018) Seasonal variations of chlorophyll *a* and environmental factors in the coastal area of the Okhotsk Sea. Nippon Suisan Gakkaishi 84:241–253

Sorokin YI, Sorokin PY (1999) Production in the Sea of Okhotsk. J Plankton Res 21:201–230

Sunda WG, Huntsman SA (1995) Iron uptake and growth limitation in oceanic and coastal phytoplankton. Mar Chem 50:189–206

Takizawa T (1982) Characteristics of the Soya Warm Current in the Okhotsk Sea. J Oceanogr Soc Jpn 38:281–292

Tammilehto A, Nielsen TG, Krock B, Moller EF, Lundholm N (2012) *Calanus* spp. —vectors for the biotoxin, domoic acid, in the Arctic marine ecosystem? Harmful Algae 20:165–174

Tanaka Y, Kajihara T (1979) The distribution of *Fulmaris glacialis* and *Puffinus tenuirostris* in the North Pacific and Okhotsk Sea during the summer. J Yamashina Inst Ornithol 11:79–86

Timmermans KR, Gerringa LJA, De Baar HJW, Van der Wagt B, Veldhuis MJW, De Jong JTM, Croot PL (2001) Growth rates of large and small Southern Ocean diatoms in relation to availability of iron in natural seawater. Limnol Oceanogr 46:260–266

Twining BS, Baines SB (2013) The trace metal composition of marine phytoplankton. Annu Rev Mar Sci 5:191–215

Yamamoto T, Tarutani K (1999) Growth and phosphate uptake kinetics of the toxic dinoflagellate *Alexandrium tamarense* from Hiroshima Bay in the Seto Inland Sea, Japan. Phycol Res 47:27–32